Exploring CPS-extrapolated DLPNO-CCSD(T_1) reference values for benchmarking DFT methods on enzymatically catalyzed reactions

Dominique A. Wappett* and Lars Goerigk*

School of Chemistry, The University of Melbourne, Victoria 3010, Australia

E-mail: dwappett@student.unimelb.edu.au; lars.goerigk@unimelb.edu.au

Abstract

Domain-based local pair natural orbital Coupled Cluster Singles Doubles with Perturbative Triples [DLPNO-CCSD(T)] is regularly used to calculate reliable benchmark reference values at a significantly lower computational cost compared to canonical CCSD(T). Recent work has shown that even greater accuracy can be obtained at only a small additional cost through extrapolation to the complete PNO space (CPS) limit. Herein we test two levels of CPS extrapolation—CPS(5,6), which approximates the accuracy of standard TightPNO, and CPS(6,7), which surpasses it—as benchmark values to test density functional approximations (DFAs) on a small set of organic and transition-metal-dependent enzyme active site models. Between the different reference levels of theory there are changes in the magnitudes of the absolute deviations for all functionals, but these are small and there is minimal impact on the relative rankings of the tested DFAs. The differences are more significant for the metalloenzymes than the organic enzymes, so we repeat the tests on our entire ENZYMES22 set of organic enzyme active site models [*J. Phys. Chem. A* **2019**, *123*, 7057.] to confirm that using the CPS extrapolations for the reference values has negligible impact on the benchmarking outcomes. This means we can particularly recommend CPS(5,6) as an alternative to standard TightPNO settings for calculating reference values, increasing the applicability of DLPNO-CCSD(T) in benchmarking reaction energies and barrier heights of larger models of organic enzymes. The DLPNO-CCSD(T)/CPS(6,7) energies for ENZYMES22 are finally presented as the updated reference values for the set, reflecting the recent improvements in the method.

1 Introduction

The popularity of Density Functional Theory[1,2] (DFT) in chemical research has led to the creation of so many density functional approximations (DFAs) that the field

has been described as a "zoo", and the popularity of a method does not always correspond with its accuracy. Trying to find one that is appropriate for a given application among the wide variety available is simplified through the process of benchmarking, which involves comparing lower-level methods to highly accurate reference data. Coupled Cluster Singles Doubles with Perturbative Triples [CCSD(T)][3] is considered the "gold standard" of chemical accuracy for theoretically calculated barrier heights and reaction energies. In practice, this is too expensive beyond small molecules, and a range of local approximations have been developed to reduce the cost of the coupled cluster treatment.[4–9] One popular method is the domain-based local pair natural orbital approximation [DLPNO-CCSD(T)],[8,9] which scales linearly with system size and can therefore be applied to much larger systems than canonical CCSD(T). The efficiency of the DLPNO approximation comes from the fact that not all electron pairs in the system are treated at the Coupled Cluster level, with a range of thresholds involved in pruning the electron pairs and pair natural orbitals (PNOs) to be included in the final correlation calculation. Three pre-defined sets of values for each threshold giving increasing levels of accuracy[10] (LoosePNO, NormalPNO and TightPNO) make the method extremely user friendly; a fourth set (VeryTightPNO) has also been created for particularly challenging applications,[11] but is less frequently used as it is not yet available as a simple keyword in the ORCA software[12–14] like the others.

DLPNO-CCSD(T)/TightPNO is regularly used to calculate reference values in benchmark studies of both organic and organometallic systems,[15–18] including our work on models of enzymatically catalyzed reactions.[19–21] Recent work has shown that the efficiency and accuracy of TightPNO calculations can be improved by altering the T_{CutPNO} parameter,[22] which determines the number of PNOs used in the correlation treatment for each electron pair—PNOs with an occupation number below the threshold value are discarded. The default value of T_{CutPNO} for TightPNO is 10^{-7}, but this can be approximated with extrapolation of values calculated with $T_{CutPNO} = 10^{-5}$ and 10^{-6} (using the TightPNO default values for all other thresholds), at a significantly reduced computational cost. On the other hand, if TightPNO calculations are feasible, then the accuracy can be improved through extrapolation of $T_{CutPNO} = 10^{-6}$ and 10^{-7} results, approximating values calculated with the tighter value of $T_{CutPNO} = 10^{-8}$. These extrapolated results have been labeled complete PNO space (CPS), similar to complete basis set (CBS) extrapolated results, as they ideally approximate the energy obtained when no PNOs are pruned ($T_{CutPNO} = 0$). The initial analysis of the CPS approaches on a range of GMTKN55[15] subsets showed that CPS(5,6) performed similarly to TightPNO against canonical CCSD(T) references (mean absolute errors (MAEs) of <0.8 kcal/mol and <0.6 kcal/mol, respectively), while CPS(6,7) was almost converged with respect to the PNO truncation error, with its residual MAE of <0.27 kcal/mol likely coming from the other sources of error in the DLPNO procedure, namely the resolution of the identity (RI) approximation and selection of strong pairs.[22] CPS(6,7) results have been shown to improve upon standard TightPNO for organometallic barrier heights[23,24] and spin state splittings.[25] The

PNO truncation error also strongly influences the size dependence of the DLPNO error, so its reduction makes a significant difference for larger systems.[26]

The accuracy of DLPNO-CCSD(T) compared to canonical CCSD(T) also improves when the newer iterative (T_1) triples procedure[27] is used instead of the original quasi-perturbative (T_0) procedure,[8] with DLPNO-CCSD(T_1) having been shown to perform better than DLPNO-CCSD(T_0) on a range of different chemical systems.[23,25,28–30]

The impact of the quality of the reference values has been shown for various benchmark sets,[15,20,31] with different references often leading to different recommendations as the magnitudes of the deviations and relative ranking of functionals change. It is therefore important to carefully consider the level of theory used to calculate the benchmarks. Our aim in this work is to assess the CPS extrapolation scheme for the calculation of reference REs and BHs associated with enzyme active site models. Previous analysis has already focused on the accuracy of CPS results in comparison to canonical CCSD(T) or other ab initio methods,[24,26] so here we look at how much the outcomes of benchmark studies change when CPS-extrapolated reference values are used instead of standard TightPNO ones. For this we use the small test set described in figure 1, which contains ten reaction energies (REs) and 4 barrier heights (BHs) across active site models of seven enzymes—these are cysteine dioxygenase (CDO), hemocyanin (Hc) and superoxide dismutase (NiSOD) from our MME55 set of metalloenzyme models,[21] and 4-oxalocrotonate tautomerase (4-OT), histone-lysine methyltransferase (HKMT), L-aspartate α-decarboxylase (AspDC) and haloalcohol dehydrogenase (HheC) from our set of mainly-organic enzymatically catalysed reactions.[19] All of these are closed shell species. Our initial work on the latter set did not assign it a name, so we adopt a modified version of the label used by Förster and Visscher in their superset for testing double hybrid DFT[32] and call the entire set ENZYMES28. ENZYMES28 additionally contained a model of the zinc-dependent enzyme phosphotriesterase (PTE), so we refer to the subset containing only the models of the four organic enzymes as ENZYMES22.We point out that all these models contain only parts of the active site, not the entire enzyme; our aim in these previous benchmark studies has been to recommend reliable DFAs for the active site region that can then be used for cluster model studies or combined with forcefield methods in layered QM/MM approaches. Geometries for all models have previously been optimised at the PBEh-3c level of theory, which contains the DFT-D3(BJ)[33,34] correction to improve the description of London dispersion interactions, and we direct the reader to the Supporting Information of Refs. 19 and 21 for the provided structures in xyz format.

We begin by using our small test set to test DLPNO-CCSD(T_1) with CPS extrapolations. We compare the BHs and REs calculated with CPS(5,6) and CPS(6,7) to standard TightPNO, and then use the three sets of values to benchmark a selection of DFAs to see how the reference level of theory impacts the perceived performance of the tested methods. Based on these results, we repeat our analysis on the entire ENZYMES22 set, and while the improvements of the CPS(6,7) extrapolation and new (T_1) triples correction are relatively small for

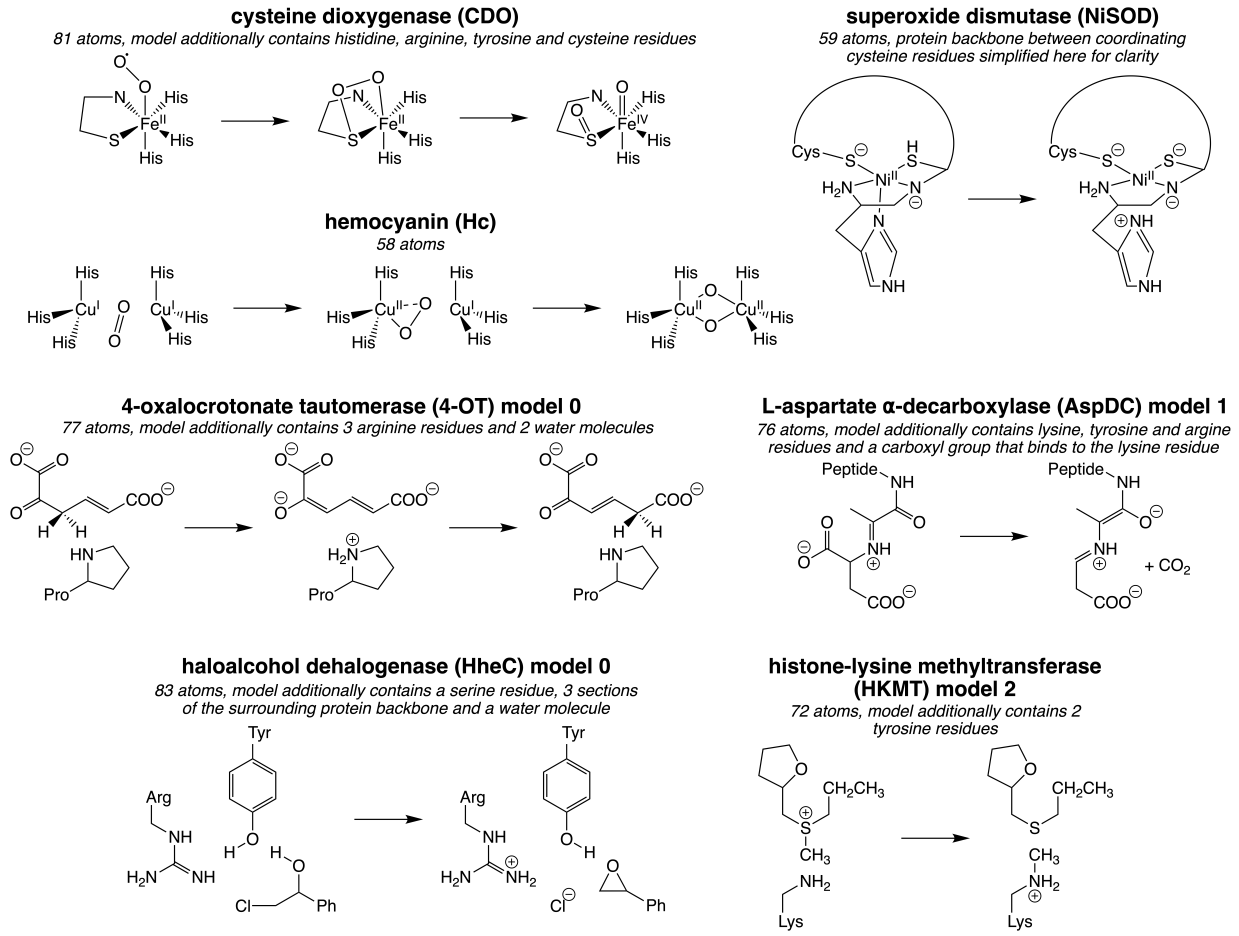

Figure 1: Schemes of the enzymatically catalyzed reaction steps used to test CPS extrapolations in this study—the test set includes the reaction energies of all steps, as well as the forward and reverse barriers of 4-OT and HKMT. The models of 4-OT, HKMT, AspDC and HheC have been taken from the ENZYMES28 set (see ref. 19 for specific details of each model system), while CDO, Hc and NiSOD have been taken from our MME55 set.[21]

these models, we present the final DLPNO-CCSD(T_1)/CPS(6,7)/CBS(3,4) REs and BHs as updated reference values for the set.

2 Computational details

All calculations in this work were done in the ORCA quantum chemistry package[12–14] (v5.0.2). The Ahlrichs-type def2-nZVPP basis sets[35] were used with all methods. Generalized Gradient Approximation (GGA), meta-GGA and meta-NGA (Nonseparable Gradient Approximation) DFT calculations were sped up with the resolution of the identity approximation for Coulomb integrals (RI-J),[36] while RI-J with the chain of spheres approximation for exchange integrals (RIJCOSX)[37] was used with the hybrid and double hybrid DFAs and the Hartree-Fock steps of the Coupled Cluster calculations. The RI-C ap-

proximation[38] was used for the MP2 steps in the double hybrid DFAs, and the Coupled Cluster calculations. These also used ORCA's default frozen core settings. The various RI approximations were used with the def2/J[39] and def2-nZVPP/C[40] auxiliary basis sets and the "GridXS2" setting for RIJCOSX. All calculations were done with the default grids and self-consistent-field (SCF) convergence thresholds.

DLPNO-CCSD(T) calculations were done with the iterative (T_1) triples correction and TightPNO settings. Additional calculations were done with the T_{CutPNO} value changed to 10^{-5} and 10^{-6}, as well as 10^{-8} for the def2-SVP and def2-TZVPP basis sets. CPS extrapolations were done following the equation:[22]

$$E_{Corr(CPS)} = E_{Corr(A)} + 1.5 \cdot (E_{Corr(B)} - E_{Corr(A)}),$$

where $E_{Corr(A)}$ is the correlation energy calculated with $T_{CutPNO} = 10^{-A}$ and $B = A + 1$. The scale factor of 1.5 is used for both CPS(5,6) and CPS(6,7) extrapolations.

Extrapolations to the CBS limit were done using the standard two-point extrapolation schemes with individual extrapolations of the SCF[41] and correlation energies:[42]

$$E_{SCF}^{(\infty)} = \frac{E_{SCF}^{(X)} \cdot exp(-\alpha\sqrt{Y}) - E_{SCF}^{(Y)} \cdot exp(-\alpha\sqrt{X})}{exp(-\alpha\sqrt{Y}) - exp(-\alpha\sqrt{X})},$$

and

$$E_{Corr}^{(\infty)} = \frac{X^\beta \cdot E_{Corr}^{(X)} - Y^\beta \cdot E_{Corr}^{(Y)}}{X^\beta - Y^\beta},$$

where X and Y are the cardinal numbers of the basis sets, and α and β are optimized constants specific to the basis sets used. For the def2-nZVPP family of basis sets, $\alpha_{CBS(2,3)} = 10.39$ and $\beta_{CBS(2,3)} = 2.40$, and $\alpha_{CBS(3,4)} = 7.88$ and $\beta_{CBS(3,4)} = 2.97$.[43]

A range of density functionals were used for an exemplary benchmark study to compare the different reference levels of theory, and the methods used are listed in table 1. Each functional was combined with the DFT-D3[33,34] and/or DFT-D4[47,80] dispersion correction where appropriate. MN15-L calculations were done using the ORCA implementation of the LibXC density functional library.[81] The non-local VV10[82] kernel in B97M-V, ωB97M-V and ωB97X-V was used in its post-SCF implementation,

Table 1: Functionals used in the example benchmark tests. References for the dispersion corrections are where the damping parameters for each functional were first presented.[a]

Name	Dispersion Correction
GGA	
BLYP[44–46]	D3(BJ),[34] D4[47]
BP86[44,48,49]	D3(BJ),[34] D4[47]
OLYP[45,46,50]	D3(BJ),[51] D4[47]
PBE[52]	D3(BJ),[34] D4[47]
revPBE 53	D3(BJ),[34] D4[47]
meta-GGA/NGA	
B97M-V[54]	[b] D3(BJ),[55] D4,[56] VV10[54]
M06L[57]	D3(0),[51] D4[47]
MN15-L[58]	D3(0)[15]
r2SCAN[59]	D3(BJ),[60] D4[60]
revTPSS[61,62]	D3(BJ),[15] D4[47]
TPSS[63]	D3(BJ),[34] D4[47]
hybrid	
B3LYP[64,65]	D3(BJ),[34] D4[47]
BHLYP[66]	D3(BJ),[51] D4[47]
CAM-B3LYP[67]	D3(BJ),[51] D4[47]
M06[68]	D3(0),[51] D4[47]
M062X[68]	D3(0),[51] D4[47]
PBEh-3c[69]	D3(BJ)[69]
ωB97M-V[70]	[b] D3(BJ),[55] D4,[56] VV10[70]
ωB97X-V[71]	VV10[71]
double hybrid	
B2PLYP[72]	D3(BJ),[51] D4[47]
DOD-SCAN-D3(BJ)[73]	D3(BJ)[73]
PWPB95[74]	D3(BJ),[51] D4[47]
revDOD-PBE-D3(BJ)[73]	D3(BJ)[73]
revDOD-PBEP86-D3(BJ)[73]	D3(BJ)[73]
revDSD-PBEP86-D3(BJ)[73]	D3(BJ)[73]
SOS0-PBE0-2[75]	D3(BJ)[76]
ωB2PLYP[77]	D3(BJ),[78] D4[78]
ωB97X-2[79]	D3(BJ)[76]

[a] D3(0): DFT-D3 with zero damping; D3(BJ): DFT-D3 with Becke-Johnson damping.
[b] The DFT-D3(BJ)/D4 dispersion correction replaces the VV10 kernel in this van-der-Waals functional, while its semi-local exchange-correlation component stays the same.

which speeds up the calculation with no impact on the results.[55] ωB97X-2 was used in its "TQZ" parameterisation.[79]

3 Results and discussion

For simplicity throughout the discussion in this paper, we refer to only standard TightPNO (with $T_{CutPNO} = 10^{-7}$) as "TightPNO"; the other approaches are all based on TightPNO with only the one threshold changed, so we label them with their T_{CutPNO} value or type of CPS extrapolation. We also use DLPNO-CCSD(T) to refer to DLPNO-CCSD(T_1) with iterative triples, and specify DLPNO-CCSD(T_0) where necessary.

For the first part of our analysis, we use the 10 REs and 4 BHs associated with the enzyme model reactions shown in figure 1 as a small test set to compare CPS(5,6) and CPS(6,7) to TightPNO as alternatives for calculating reference values for DFT benchmarking. We note that the loosened values of T_{CutPNO} (10^{-5} and 10^{-6}) should not be used outside the CPS extrapolation scheme as they compromise the accuracy of TightPNO significantly. Similarly, CBS(2,3) results are unreliable due to the poor accuracy of the double-ζ basis set negatively affecting the extrapolation. While we do not consider these lower-level approaches as potential benchmark strategies in the subsequent DFA tests, they are useful for observing trends across the REs and BHs with the T_{CutPNO} values, and the CBS(2,3) results allow us to compare CPS(6,7) to the tightened value of $T_{CutPNO} = 10^{-8}$, which could not be done for CBS(3,4) as the def2-QZVPP calculations were computationally too expensive. We also note that the CPS(5,6) and TightPNO results at the CBS(3,4) level for the metalloenzymes CDO, Hc and NiSOD have been taken from the brief tests we conducted when selecting the reference values for our new MME55 set,[21] where CPS(5,6) was referred to as "estimated TightPNO".

In figure 2 we show DLPNO-CCSD(T) energies of the small test set calculated with a range of T_{CutPNO} values for both CBS(2,3) and CBS(3,4). Between these, the trends are mostly the same, with similarly shaped dependence of the REs and BHs on T_{CutPNO} at both levels. The CPS extrapolations generally fit the trends well, with CPS(5,6) in between 10^{-6} and 10^{-7} and CPS(6,7) lying beyond 10^{-7}. In some cases like 4-OT RE1 and HKMT-2 RBH, CPS(5,6) overshoots the TightPNO/10^{-7} energy due to the strong inaccuracy of $T_{CutPNO} = 10^{-5}$, similar to CBS(2,3) being affected by the low quality of double-ζ results. CPS(6,7) is more consistent, and generally represents an improvement over standard TightPNO in terms of approximating the tighter $T_{CutPNO} = 10^{-8}$ threshold value. As relative energies do not necessarily converge monotonically to the $T_{CutPNO} = 0$ limit, we also show the convergence of the correlation energies of each structure in this small test set with the T_{CutPNO} values in figure S2 of the Supporting Information. The observed behavior is generally different between CBS(2,3) and CBS(3,4), but this is unlikely to be an issue as Altun et al. have noted that the form of the CPS extrapolation does not depend on the form of the convergence of the correlation energies.[22]

From these tested BHs and REs, we have calculated mean (absolute) deviations (MDs and MADs) of the CPS and standard TightPNO results as a rough es-

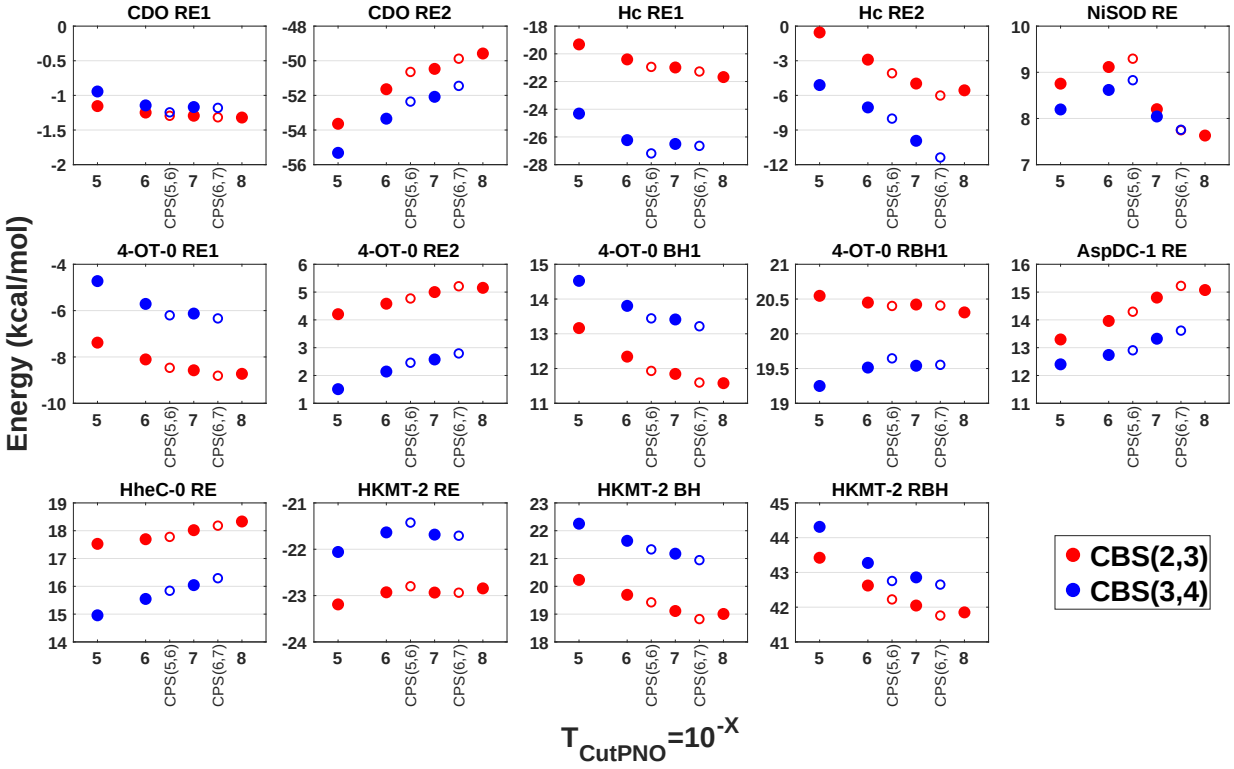

Figure 2: Dependence of the DLPNO-CCSD(T)/CBS reaction energies and barrier heights on T_{CutPNO} for the small test set (figure 1). A value of 10^{-7} is the default for TightPNO. Tightened $T_{CutPNO} = 10^{-8}$ results could not be obtained for CBS(3,4) due to the cost of the def2-QZVPP calculations.

timate of their accuracy, and these are presented in figure 3. At the CBS(2,3) level, we compare these to the $T_{CutPNO} = 10^{-8}$ results, and see that CPS(6,7) is indeed closer than TightPNO as expected (MADs of 0.16 and 0.32 kcal/mol, respectively), while CPS(5,6) has an MAD of 0.59 kcal/mol. The MDs also get closer to zero, with the MD of CPS(6,7) having a very slightly negative MD due to cases like Hc RE2 and the HKMT-2 barrier heights where CPS(6,7) slightly overshoots the $T_{CutPNO} = 10^{-8}$ energy (as seen in figure 2). There are also reductions in the largest deviations by magnitude. For CPS(5,6), the largest deviation is 1.66 kcal/mol, with two more deviations also larger than the generally accepted 1 kcal/mol chemical accuracy limit for REs and BHs; for TightPNO and CPS(6,7) the largest deviations are −0.89 kcal/mol and 0.45 kcal/mol, respectively. For CBS(3,4), comparison of CPS(5,6) to TightPNO shows that the lower-level extrapolation can replicate standard TightPNO results with an MAD of 0.37 kcal/mol at a significantly reduced cost. In our development of the MME55 benchmark set we have already noted that CPS(5,6) deviates significantly (1.92 kcal/mol) from TightPNO for RE2 of the copper-dependent enzyme Hc due to issues with the specific geometry formed in this step;[21] across the rest of the test set used here all deviations are below 0.8

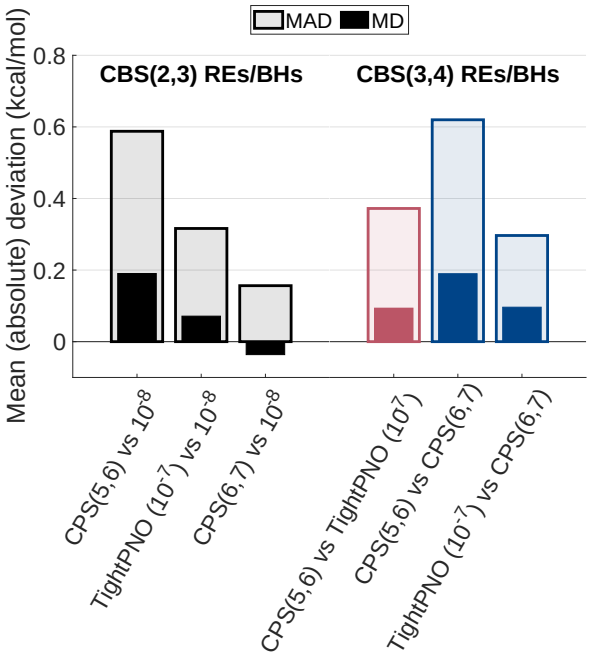

Figure 3: Mean absolute deviations of various DLPNO-CCSD(T) levels of theory across the small test set (figure 1). At the CBS(2,3) level the CPS approaches and TightPNO are compared to $T_{CutPNO} = 10^{-8}$; for CBS(3,4) results, CPS(5,6) is compared to TightPNO, and both of those are compared to CPS(6,7).

kcal/mol and the MAD is 0.22 kcal/mol, so for most larger systems where standard TightPNO is unfeasible, CPS(5,6) can therefore be considered a possible alternative. The MAD of CPS(5,6) increases to 0.62 kcal/mol when compared to the more accurate CPS(6,7) results, while TightPNO itself has a MAD of 0.30 kcal/mol. These are also inflated slightly by the Hc RE2 deviations being more than twice that of the second largest deviation (3.37 kcal/mol followed by 1.07 kcal/mol for CPS(5,6), and 1.45 kcal/mol followed by −0.63 kcal/mol for TightPNO). Given that CPS(6,7) also has its own level of error, we expect that a comparison to tightened T_{CutPNO} results at the CBS(3,4) level would give slightly higher MADs for CPS(5,6) and standard TightPNO, but they are unlikely to be above the 1 kcal/mol chemical accuracy limit for REs and BHs, particularly for the systems other than Hc.

In a benchmark study the performance of a functional is determined by the deviations from the reference values, calculated as $\mathrm{RE/BH}_{DFA} - \mathrm{RE/BH}_{ref.}$, so we can test the applicability of the CPS extrapolation approach for calculating benchmarks through the observed changes in MADs of a selected set of DFAs when each level of theory is used as the reference method. For the DFAs listed in table 1 we calculate three sets of MADs using our reference levels of theory of interest: DLPNO-CCSD(T)/CBS(3,4) with either CPS(5,6), standard TightPNO or CPS(6,7) (in order of increasing accuracy). Our main analysis herein focuses on the results for the DFAs in their DFT-D3-corrected (or VV10-corrected, where applicable) forms, while results of the functionals plain and with DFT-D4 are given in the Supporting Information.

Figure 4 shows the MADs of the tested DFAs against the three sets of references for the whole test set, as well as mean MADs (MMADs) for each rung of Jacob's ladder for the metalloenzymes and organic enzymes separately. Note that the MMADs are calculated from all functional MADs including those for the plain and DFT-D4 corrected methods, not just the DFT-D3 results; plots of the MADs of all plain and D4-corrected DFAs are given in figure S4 in the Supporting Information. Looking first at the overall results, we see that the MADs of all hybrid functionals increase as the references get more accurate,

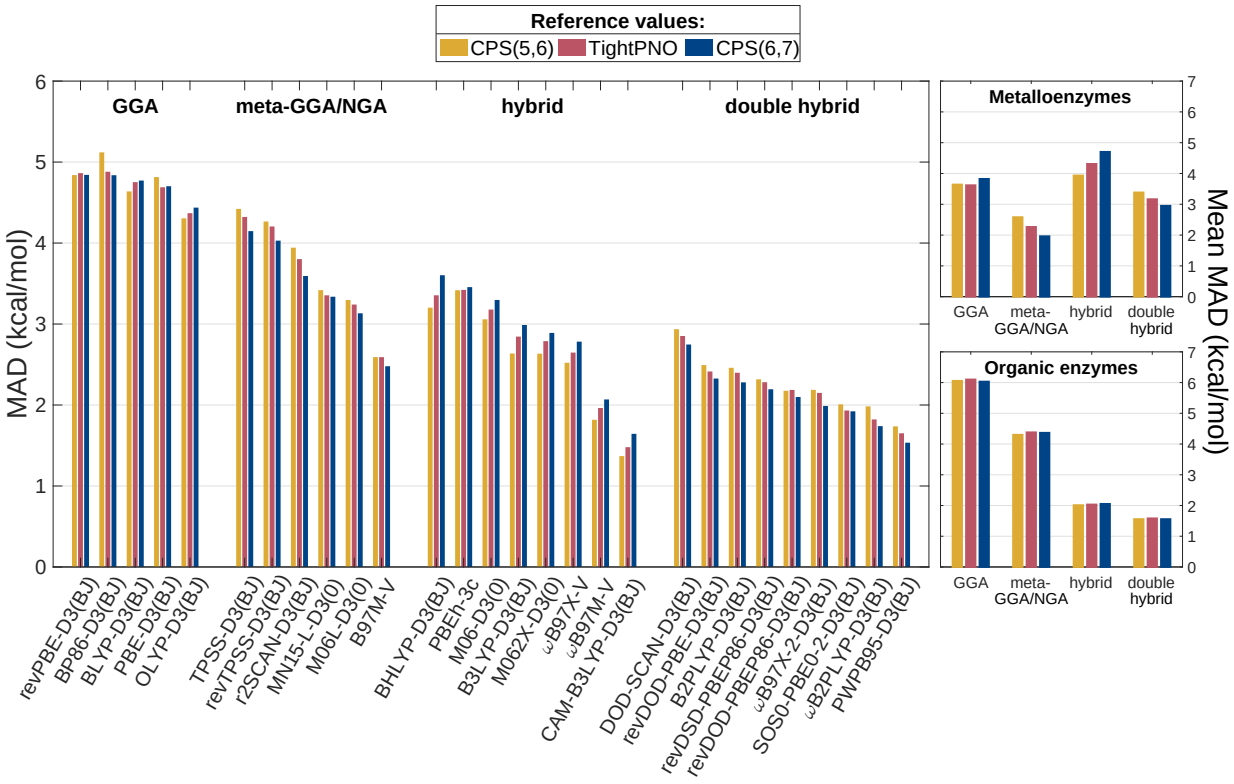

Figure 4: MADs of each functional against DLPNO-CCSD(T)/CBS references with either CPS(5,6), TightPNO or CPS(6,7), across the small test set (figure 1). Within each class of DFA, functionals are ordered from largest to smallest CPS(6,7) MADs. Additional plots show mean MADs within rungs of Jacob's ladder calculated separately for the organic enzymes and metalloenzymes in the small test set.

while for the meta-GGA/NGA functionals and double hybrids they decrease and the results are mixed for the GGAs. Most functionals have a monotonic trend with the T_{CutPNO} accuracy, but in general the changes are rather small. Even for the hybrid functionals which see the largest differences, the average MAD increase is only 0.15 kcal/mol for each step up in reference accuracy. There are also only a few changes in the relative rankings of the functionals. Within the rungs, OLYP-D3(BJ) is always the best GGA but the others rearrange with different choices of reference value, and BHLYP-D3(BJ) overtakes PBEh-3c to become the worst hybrid when going from TightPNO to CPS(6,7) references. The most notable difference is in the comparison of the best hybrids to the double hybrids. Against CPS(5,6) references, the best 3 DFAs are CAM-B3LYP-D3(BJ), PWPB95-D3(BJ) and ωB97M-V; going up to CPS(6,7) causes PWPB95-D3(BJ) and CAM-B3LYP-D3(BJ) to swap places, and multiple double hybrid DFAs overtake ωB97M-V. Looking at other statistical values (figure S3 and tables S8–S10 in the Supporting Information), some clear changes in the hybrid DFA rankings based on the error ranges are observed, typically

when a RE or BH that is more strongly affected by the reference values has the maximum or minimum deviation, but the impact of the references on the MDs, RMSDs and MAPDs is also minimal.

Transition metals are often harder to treat computationally and results for organometallic systems typically have larger errors, so we expect that the difference in the DLPNO-CCSD(T) approaches will be stronger for the metalloenzymes than the organic enzymes, and indeed this is observed in the subset MMADs in figure 4. For each rung, the MMAD is much less sensitive to the choice of reference level of theory for the organic enzymes than the metalloenzymes, with the hybrid MMAD increasing by 0.4 kcal/mol with each step up in reference accuracy for the metalloenzymes, but less than 0.1 kcal/mol across all three levels for the organic enzymes. Subset MADs for all DFT-D3-corrected functionals are shown in figure S5 in the Supporting Information, and we note that some of the hybrid DFAs (such as CAM-B3LYP-D3(BJ), M062X-D3(0) and BHLYP-D3(BJ)) see differences in their MADs of around 1 kcal/mol between the two CPS-extrapolated levels of theory, while there are a few more observed rearrangements in the functional rankings as well. The behavior seen in the overall results, with the MADs of the hybrids increasing and double hybrids decreasing with the accuracy of the references, is not observed for the organic enzymes as it is mostly due to Hc RE2. As shown in figure 2, this RE gets more negative across our three reference levels of theory; as the deviations are calculated $RE_{DFA} - RE_{ref.}$, the lower references make the deviations more positive. This results in increased magnitudes for the hybrids, which already have positive deviations at the CPS(5,6) level, while the negative deviations of the double hybrids shift closer to zero.

Overall, all three reference levels of theory give relatively similar benchmarking outcomes. For metalloenzymes, which are more sensitive to the choice of reference value, we recommend CPS(6,7) as a low cost way of improving the accuracy of DLPNO-CCSD(T) in terms of reducing the PNO truncation error—if TightPNO calculations are feasible for a system, then so is CPS(6,7) as the additional $T_{CutPNO} = 10^{-6}$ calculations are significantly more computationally efficient. The relative rankings of the DFAs are not significantly impacted, however, when CPS(5,6) is used instead of TightPNO. The CPS(5,6) BHs and REs are not necessarily converged with respect to T_{CutPNO} so they may not be adequate for high level analysis of specific enzyme energetics, but this level of theory is a reasonable option for an assessment of density functionals when lower cost methods are required. This is particularly useful in extending the applicability of DLPNO-CCSD(T) to benchmark sets containing larger systems. For organic enzymes, any changes in the performance of the DFAs with the three reference levels of theory seem to be negligible. We therefore conduct further analysis using the entire ENZYMES22 set, to see whether this holds across a larger set. As well as the models of 4-OT, AspDC, HheC and HKMT included in the small test set, ENZYMES22 contains additional models of AspDC (one smaller and one larger model), HheC (one larger model) and HKMT (two smaller models); all of these follow the same mechanisms shown in figure 1. This extends the range of system sizes represented in our tests in both directions, with ENZYMES22 con-

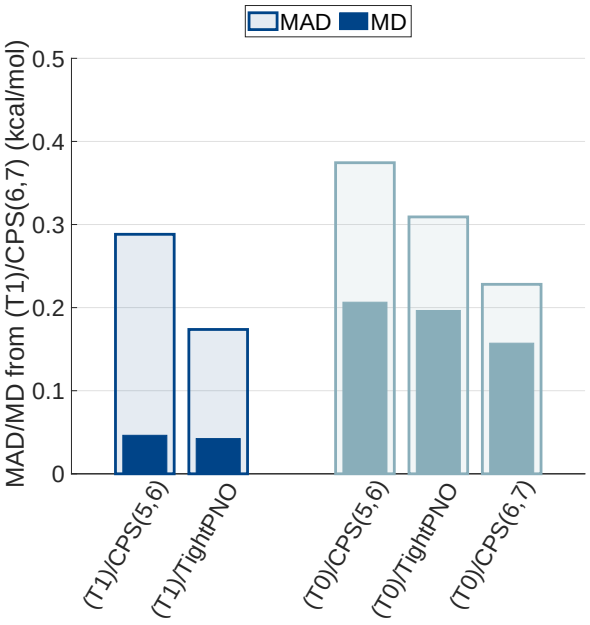

Figure 5: MADs (kcal/mol) of Coupled Cluster approaches against DLPNO-CCSD(T_1)/CPS(6,7) across the ENZYMES22 set. All results are at the CBS(3,4) level.

taining models from 27 to 112 atoms.

For the following analysis on ENZYMES22, all values are at the CBS(3,4) level. The reference values we presented for these models in 2019[19,83] were based on DLPNO-CCSD(T_0) with the older, non-iterative triples correction, so as well as an initial comparison of CPS(5,6) and TightPNO to CPS(6,7), figure 5 also compares DLPNO-CCSD(T_0) to DLPNO-CCSD(T) with iterative triples as used herein. Looking first at the DLPNO-CCSD(T)-based approaches, we see that CPS(5,6) (MAD of 0.29 kcal/mol and largest deviation by magnitude of −0.71 kcal/mol) is again less accurate than standard TightPNO (MAD of 0.17 kcal/mol and largest deviation of −0.33 kcal/mol), but the MADs are relatively small, and both MDs are very similar. The (T_0) triples correction increases the deviations of standard TightPNO and the two CPS-extrapolated alternatives, with DLPNO-CCSD(T_0)/CPS(6,7) having an MAD of 0.2 kcal/mol and largest deviation of 0.57 kcal/mol compared to DLPNO-CCSD(T)/CPS(6,7). While the difference between the triples corrections is not significantly large here, we still prioritise the use of the newer (T_1) correction as it is theoretically more rigorous.

It is too expensive to use tighter T_{CutPNO} thresholds for most models in ENZYMES22, but we have also briefly looked at results using $T_{CutPNO} = 10^{-8}$ and $T_{CutPNO} = 10^{-9}$ for the two smallest models in section S3.1.1 of the Supporting Information as an additional test of the accuracy of CPS(6,7). We see similar trends in the correlation energies for each structure as well as REs and BHs to those seen for the small test set in figures S2 and 2. While the REs and BHs do not appear to fully reach convergence within the range tested, the changes in energy beyond CPS(6,7) are small. At the CBS(3,4) level, CPS(6,7) has an average difference from $T_{CutPNO} = 10^{-8}$ of 0.06 kcal/mol across the 6 energies associated with AspDC model 0 and HKMT model 0, with the largest difference being only 0.13 kcal/mol. For HKMT model 0 $T_{CutPNO} = 10^{-9}$ values could also be achieved, and CPS(6,7) differed by less than 0.1 kcal/mol for all three energies.

Using the three sets of reference values to test the DFAs as before, we show results for the whole ENZYMES22 set in figure 6. As seen for the subset used in the test set previously, the differences in the MADs with the three reference lev-

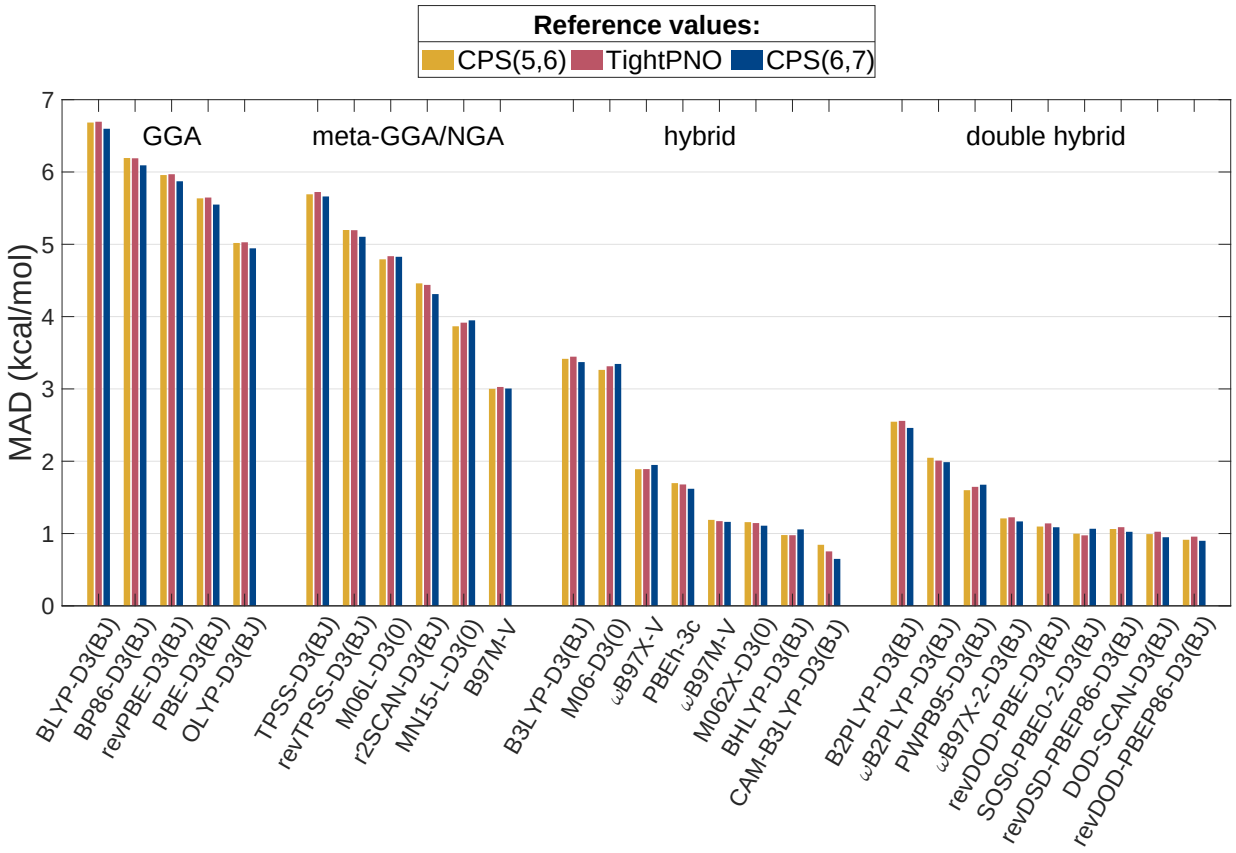

Figure 6: MADs of each functional against DLPNO-CCSD(T)/CBS references with either CPS(5,6), TightPNO or CPS(6,7), across the ENZYMES22 set. Within each class of DFA, functionals are ordered from largest to smallest CPS(6,7) MADs.

els of theory are negligible, and no significant changes in the functional rankings are observed. This holds across all statistics, including for the plain and DFT-D4-corrected DFAs, and is observed even when the BHs and REs are considered separately (all statistical values for the entire set, as well as the BH and RE subsets separately, are given in sections S3.3 and S3.4 of the Supporting Information). Based on these results we can conclude that for models of organic enzymes and their associated BHs and REs, the additional accuracy of CPS(6,7) is not required, and the lower-cost alternative CPS(5,6) is accurate enough to use as reference values for large models—extending the limits of system sizes on which we can conduct reliable benchmark studies. We also briefly note the strong performance of CAM-B3LYP-D3(BJ), which was not previously tested in our original study using the ENZYMES28 set. This is a notable and surprising result, as it has not been shown to be particularly better compared to global hybrids in a more comprehensive study of main-group thermochemistry.[51]

We conclude this work by presenting the DLPNO-CCSD(T_1)/CPS(6,7)/CBS(3,4) reference values (table 2) for the ENZYMES22 set calculated herein so that they can be used for future benchmarking

Table 2: DLPNO-CCSD(T_1)/CPS(6,7)/CBS(3,4) reference values for the ENZYMES22 set alongside the DLPNO-CCSD(T_0)-based values previously published in Refs. 19 and 83. All values in kcal/mol.

Enzyme model	Size (no. atoms)	Energy	Old ref. value	CPS(6,7) ref. value
4-OT 0	77	RE1	−4.90	−6.34
4-OT 0	77	RE2	1.25	2.79
4-OT 0	77	BH1	14.39	13.22
4-OT 0	77	RBH1	19.29	19.55
AspDC 0	27	RE	−5.50	−5.55
AspDC 0	27	BH	4.10	3.98
AspDC 0	27	RBH	9.60	9.53
AspDC 1	76	RE	13.03	13.61
AspDC 2	95	RE	3.67	4.33
HheC 0	83	RE	16.05	16.29
HheC 1	112	RE	14.06	14.51
HheC 1	112	BH	17.64	17.15
HheC 1	112	RBH	3.58	2.64
HKMT 0	29	RE	−5.67	−5.38
HKMT 0	29	BH	26.05	26.16
HKMT 0	29	RBH	31.72	31.53
HKMT 1	46	RE	−1.99	−1.61
HKMT 1	46	BH	27.83	27.90
HKMT 1	46	RBH	29.82	29.52
HKMT 2	72	RE	−21.53	−21.71
HKMT 2	72	BH	21.42	20.94
HKMT 2	72	RBH	42.95	42.65

work on these models; although most values are not significantly impacted by the new triples correction and CPS extrapolation, we use this opportunity to formally update the set to reflect the recent improvements in the DLPNO-CCSD(T) methodology. The average difference between these values and the previously published DLPNO-CCSD(T_0)/TightPNO-based references is 0.47 kcal/mol, with the largest impact seen for the larger models: 4-OT (three of the four energies change by more than 1 kcal/mol), the RBH of HheC model 1 (0.94 kcal/mol) and the RE of AspDC model 2 (0.66 kcal/mol).

We provide a comparison of the functional MADs calculated from the old DLPNO-CCSD(T_0)/TightPNO-based references and new DLPNO-CCSD(T_1)/CPS(6,7)/CBS(3,4) references in figure S11 of the Supporting Information, and note some minor changes in the DFA rankings. Against the old references, SOS0-PBE0-2-D3(BJ) was clearly the best double hybrid but it is almost indistinguishable from the (rev)DOD/DSD functionals when compared to the updated references, while CAM-B3LYP-D3(BJ) was not as separated from the other best hybrids against the old references as it is against the new ones. However we note that the best hybrids and double hybrids all perform well against both sets of references, with MADs generally around 1 kcal/mol, so small differences in the magnitudes and rankings are unlikely to be statistically significant and a number of the tested methods can be recommended as reliable.

4 Summary and conclusions

Herein we have tested the complete PNO space extrapolation approach as a low-cost way of altering the accuracy and efficiency of DLPNO-CCSD(T_1), so that it can be used to calculate reference values for benchmarking enzymatically catalyzed reactions. For this we have used a test set of 10 REs and 4 BHs representing both organic and metalloenzymes, taken from previous benchmark studies for which DLPNO-CCSD($T_{1/0}$)/TightPNO references had been used. CPS(5,6) extrapolated results approach the accuracy of TightPNO (which has a default value of $T_{CutPNO} = 10^{-7}$) but do not fully replicate it; similarly CPS(6,7) approaches results calculated with a tightened T_{CutPNO} value of 10^{-8}, surpassing TightPNO with

only the additional cost of the much more efficient $T_{CutPNO} = 10^{-6}$ calculation. Using these three levels of theory as benchmarks to test DFAs, we see only minor changes in the MADs with the reference quality. The effect is more significant for the metalloenzymes, but even with changes of up to 0.5 kcal/mol in the MADs with each step up in the reference level of theory, there are only few significant changes in the relative rankings of the DFAs. To further investigate the results for models of organic enzymes, for which the differences in the MADs appeared to be negligible, we extend the analysis to the ENZYMES22 set of enzymatically catalyzed reactions. Even across this larger set we see no significant difference in the benchmarking outcomes across the three tested reference levels of theory. We therefore conclude that the CPS extrapolation technique can be useful for calculating reference REs and BHs associated with enzyme active site models—particularly in the case of CPS(5,6), which gives similar results to standard TightPNO at a significantly reduced cost, allowing DLPNO-CCSD(T) to be used as a benchmark level of theory for larger systems. We also present the final DLPNO-CCSD(T_1)/CPS(6,7)/CBS(3,4) REs and BHs to be used as updated reference values for the ENZYMES22 set in further benchmarking work.

Supporting Information Available

The Supporting Information is available free of charge at https://pubs.acs.org/doi/.

DLPNO-CCSD(T_1) and DFT energies for all systems; detailed benchmarking results of all tested DFT methods for the small test set and ENZYMES22.

Acknowledgement D. A. Wappett acknowledges an Australian Government Research Training Program Scholarship. We are thankful for the allocation of computing resources by the National Computational Infrastructure (NCI) National Facility within the National Computational Merit Allocation Scheme (Project No. fk5) and The University of Melbourne's Research Computing Services and the Petascale Campus Initiative (Project No. punim0094). This research was additionally supported by the Research Computing Services NCI Access scheme at The University of Melbourne.

References

(1) Hohenberg, P.; Kohn, W. Inhomogeneous Electron Gas. *Phys. Rev. B* **1964**, *136*, 864–871.

(2) Kohn, W.; Sham, L. J. Self-Consistent Equations Including Exchange and Correlation Effects. *Phys. Rev.* **1965**, *140*, A1133–A1138.

(3) Raghavachari, K.; Trucks, G. W.; Pople, J. A.; Head-Gordon, M. A Fifth-Order Perturbation Comparison of Electron Correlation Theories. *Chem. Phys. Lett.* **1989**, *157*, 479–483.

(4) Ma, Q.; Werner, H.-J. Explicitly Correlated Local Coupled-cluster Methods Using Pair Natural Orbitals. *Wiley Interdiscip. Rev.: Comput. Mol. Sci.* **2018**, *8*.

(5) Ma, Q.; Werner, H.-J. Scalable Electron Correlation Methods. 5. Parallel Perturbative Triples Correction for Explicitly Correlated Local Coupled Cluster with Pair Natural Orbitals. *J. Chem. Theory Comput.* **2018**, *14*, 198–215.

(6) Nagy, P. R.; Samu, G.; Kállay, M. Optimization of the Linear-Scaling Local Natural Orbital CCSD(T) Method: Improved Algorithm and Benchmark Applications. *J. Chem. Theory Comput.* **2018**, *14*, 4193–4215.

(7) Nagy, P. R.; Kállay, M. Approaching the Basis Set Limit of CCSD(T) Energies for Large Molecules with Local Natural Orbital Coupled-Cluster Methods. *J. Chem. Theory Comput.* **2019**, *15*, 5275–5298.

(8) Riplinger, C.; Sandhoefer, B.; Hansen, A.; Neese, F. Natural Triple Excitations in Local Coupled Cluster Calculations with Pair Natural Orbitals. *J. Chem. Phys.* **2013**, *139*, 134101.

(9) Riplinger, C.; Pinski, P.; Becker, U.; Valeev, E. F.; Neese, F. Sparse Maps—A Systematic Infrastructure for Reduced-Scaling Electronic Structure Methods. II. Linear Scaling Domain Based Pair Natural Orbital Coupled Cluster Theory. *J. Chem. Phys.* **2016**, *144*, 024109.

(10) Liakos, D. G.; Sparta, M.; Kesharwani, M. K.; Martin, J. M. L.; Neese, F. Exploring the Accuracy Limits of Local Pair Natural Orbital Coupled-Cluster Theory. *J. Chem. Theory Comput.* **2015**, *11*, 1525–1539.

(11) Pavošević, F.; Peng, C.; Pinski, P.; Riplinger, C.; Neese, F.; Valeev, E. F. SparseMaps—A Systematic Infrastructure for Reduced Scaling Electronic Structure Methods. V. Linear Scaling Explicitly Correlated Coupled-Cluster Method with Pair Natural Orbitals. *J. Chem. Phys.* **2017**, *146*, 174108.

(12) Neese, F. The ORCA Program System. *Wiley Interdiscip. Rev.: Comput. Mol. Sci.* **2012**, *2*, 73–78.

(13) Neese, F. Software Update: The ORCA Program System, Version 4.0. *Wiley Interdiscip. Rev.: Comput. Mol. Sci.* **2018**, *8*.

(14) Neese, F.; Wennmohs, F.; Becker, U.; Riplinger, C. The ORCA Quantum Chemistry Program Package. *J. Chem. Phys.* **2020**, *152*, 224108.

(15) Goerigk, L.; Hansen, A.; Bauer, C.; Ehrlich, S.; Najibi, A.; Grimme, S. A Look at the Density Functional Theory Zoo with the Advanced GMTKN55 Database for General Main Group Thermochemistry, Kinetics and Noncovalent iInteractions. *Phys. Chem. Chem. Phys.* **2017**, *19*, 32184–32215.

(16) Dohm, S.; Hansen, A.; Steinmetz, M.; Grimme, S.; Checinski, M. P. Comprehensive Thermochemical Benchmark Set of Realistic Closed-Shell Metal Organic Reactions. *J. Chem. Theory Comput.* **2018**, *14*, 2596–2608.

(17) Iron, M. A.; Janes, T. Evaluating Transition Metal Barrier Heights with the Latest Density Functional

Theory Exchange-Correlation Functionals: The MOBH35 Benchmark Database. *J. Phys. Chem. A* **2019**, *123*, 3761–3781.

(18) Prasad, V. K.; Pei, Z.; Edelmann, S.; Otero-de-la-Roza, A.; DiLabio, G. A. BH9, a New Comprehensive Benchmark Data Set for Barrier Heights and Reaction Energies: Assessment of Density Functional Approximations and Basis Set Incompleteness Potentials. *J. Chem. Theory Comput.* **2022**, *18*, 151–166.

(19) Wappett, D. A.; Goerigk, L. Toward a Quantum-Chemical Benchmark Set for Enzymatically Catalyzed Reactions: Important Steps and Insights. *J. Phys. Chem. A* **2019**, *123*, 7057–7074.

(20) Wappett, D. A.; Goerigk, L. A Guide to Benchmarking Enzymatically Catalysed Reactions: The Importance of Accurate Reference Energies and the Chemical Environment. *Theor. Chem. Acc.* **2021**, *140*, 68.

(21) Wappett, D. A.; Goerigk, L. Benchmarking Density Functional Theory Methods for Metalloenzyme Reactions: The Introduction of the MME55 Set. *J. Chem. Theory Comput.* **2023**, published online, DOI: 10.1021/acs.jctc.3c00558 (accessed on 25 November 2023.

(22) Altun, A.; Neese, F.; Bistoni, G. Extrapolation to the Limit of a Complete Pair Natural Orbital Space in Local Coupled-Cluster Calculations. *J. Chem. Theory Comput.* **2020**, *16*, 6142–6149.

(23) Semidalas, E.; Martin, J. M. The MOBH35 Metal–Organic Barrier Heights Reconsidered: Performance of Local-Orbital Coupled Cluster Approaches in Different Static Correlation Regimes. *J. Chem. Theory Comput.* **2022**, *18*, 883–898.

(24) Altun, A.; Riplinger, C.; Neese, F.; Bistoni, G. Exploring the Accuracy Limits of PNO-Based Local Coupled-Cluster Calculations for Transition-Metal Complexes. *J. Chem. Theory Comput.* **2023**, *19*, 2039–2047.

(25) Drosou, M.; Mitsopoulou, C. A.; Pantazis, D. A. Reconciling Local Coupled Cluster with Multireference Approaches for Transition Metal Spin-State Energetics. *J. Chem. Theory Comput.* **2022**, *18*, 3538–3548.

(26) Altun, A.; Ghosh, S.; Riplinger, C.; Neese, F.; Bistoni, G. Addressing the System-Size Dependence of the Local Approximation Error in Coupled-Cluster Calculations. *J. Phys. Chem. A* **2021**, *125*, 9932–9939.

(27) Guo, Y.; Riplinger, C.; Becker, U.; Liakos, D. G.; Minenkov, Y.; Cavallo, L.; Neese, F. Communication: An Improved Linear Scaling Perturbative Triples Correction for the Domain Based Local Pair-Natural Orbital Based Singles and Doubles Coupled Cluster Method [DLPNO-CCSD(T)]. *J. Chem. Phys.* **2018**, *148*, 011101.

(28) Liakos, D. G.; Guo, Y.; Neese, F. Comprehensive Benchmark Results for the Domain Based Local Pair Natural Orbital Coupled Cluster Method

(DLPNO-CCSD(T)) for Closed- and Open-Shell Systems. *J. Phys. Chem. A* **2020**, *124*, 90–100.

(29) Sylvetsky, N.; Banerjee, A.; Alonso, M.; Martin, J. M. L. Performance of Localized Coupled Cluster Methods in a Moderately Strong Correlation Regime: Hückel–Möbius Interconversions in Expanded Porphyrins. *J. Chem. Theory Comput.* **2020**, *16*, 3641–3653.

(30) Efremenko, I.; Martin, J. M. L. Coupled Cluster Benchmark of New DFT and Local Correlation Methods: Mechanisms of Hydroarylation and Oxidative Coupling Catalyzed by Ru(II, III) Chloride Carbonyls. *J. Phys. Chem. A* **2021**, *125*, 8987–8999.

(31) Karton, A.; Goerigk, L. Accurate Reaction Barrier Heights of Pericyclic Reactions: Surprisingly Large Deviations for the CBS-QB3 Composite Method and Their Consequences in DFT Benchmark Studies. *J. Comput. Chem.* **2015**, *36*, 622–632.

(32) Förster, A.; Visscher, L. Double Hybrid DFT Calculations with Slater Type Orbitals. *J. Comput. Chem.* **2020**, *41*, 1660–1684.

(33) Grimme, S.; Antony, J.; Ehrlich, S.; Krieg, H. A Consistent and Accurate *Ab Initio* Parametrization of Density Functional Dispersion Correction (DFT-D) for the 94 Elements H-Pu. *J. Chem. Phys.* **2010**, *132*, 154104.

(34) Grimme, S.; Ehrlich, S.; Goerigk, L. Effect of the Damping Function in Dispersion Corrected Density Functional Theory. *J. Comput. Chem.* **2011**, *32*, 1456–1465.

(35) Weigend, F.; Ahlrichs, R. Balanced Basis Sets of Split Valence, Triple Zeta Valence and Quadruple Zeta Valence Quality for H to Rn: Design and Assessment of Accuracy. *Phys. Chem. Chem. Phys.* **2005**, *7*, 3297.

(36) Vahtras, O.; Almlöf, J.; Feyereisen, M. Integral Approximations for LCAO-SCF Calculations. *Chem. Phys. Lett.* **1993**, *213*, 514–518.

(37) Izsák, R.; Neese, F. An Overlap Fitted Chain of Spheres Exchange Method. *J. Chem. Phys.* **2011**, *135*, 144105.

(38) Feyereisen, M.; Fitzgerald, G.; Komornicki, A. Use of Approximate Integrals in Ab Initio Theory. An Application in MP2 Energy Calculations. *Chem. Phys. Lett.* **1993**, *208*, 359–363.

(39) Weigend, F. Accurate Coulomb-fitting Basis Sets for H to Rn. *Phys. Chem. Chem. Phys.* **2006**, *8*, 1057.

(40) Hellweg, A.; Hättig, C.; Höfener, S.; Klopper, W. Optimized Accurate Auxiliary Basis Sets for RI-MP2 and RI-CC2 Calculations for the Atoms Rb to Rn. *Theor. Chem. Acc.* **2007**, *117*, 587–597.

(41) Karton, A.; Martin, J. M. L. Comment on: "Estimating the Hartree-Fock Limit from Finite Basis Set Calculations" [Jensen F (2005) Theor Chem Acc 113:267]. *Theor. Chem. Acc.* **2006**, *115*, 330–333.

(42) Halkier, A.; Helgaker, T.; Jørgensen, P.; Klopper, W.; Koch, H.; Olsen, J.; Wilson, A. K. Basis-Set Convergence in Correlated Calculations on Ne, N_2, and H_2O. *Chem. Phys. Lett.* **1998**, *286*, 243–252.

(43) Neese, F.; Hansen, A.; Liakos, D. G. Efficient and Accurate Approximations to the Local Coupled Cluster Singles Doubles Method Using a Truncated Pair Natural Orbital Basis. *J. Chem. Phys.* **2009**, *131*, 064103.

(44) Becke, A. D. Density-Functional Exchange-Energy Approximation With Correct Asymptotic Behavior. *Phys. Rev. A* **1988**, *38*, 3098–3100.

(45) Lee, C.; Yang, W.; Parr, R. G. Development of the Colle-Salvetti Correlation-Energy Formula into a Functional of the Electron Density. *Phys. Rev. B* **1988**, *37*, 785–789.

(46) Miehlich, B.; Savin, A.; Stoll, H.; Preuss, H. Results Obtained with the Correlation Energy Density Functionals of Becke and Lee, Yang and Parr. *Chem. Phys. Lett.* **1989**, *157*, 200–206.

(47) Caldeweyher, E.; Ehlert, S.; Hansen, A.; Neugebauer, H.; Spicher, S.; Bannwarth, C.; Grimme, S. A Generally Applicable Atomic-Charge Dependent London Dispersion Correction. *J. Chem. Phys.* **2019**, *150*, 154122.

(48) Perdew, J. P. Density-Functional Approximation for the Correlation Energy of the Inhomogeneous Electron Gas. *Phys. Rev. B* **1986**, *33*, 8822–8824.

(49) Perdew, J. P. Erratum: Density-Functional Approximation for the Correlation Energy of the Inhomogeneous Electron Gas. *Phys. Rev. B* **1986**, *34*, 7406–7406.

(50) Handy, N. C.; Cohen, A. J. Left-Right Correlation Energy. *Mol. Phys.* **2001**, *99*, 403–412.

(51) Goerigk, L.; Grimme, S. A Thorough Benchmark of Density Functional Methods for General Main Group Thermochemistry, Kinetics, and Noncovalent Interactions. *Phys. Chem. Chem. Phys.* **2011**, *13*, 6670.

(52) Perdew, J. P.; Burke, K.; Ernzerhof, M. Generalized Gradient Approximation Made Simple. *Phys. Rev. Lett.* **1996**, *77*, 3865–3868.

(53) Zhang, Y.; Yang, W. Comment on "Generalized Gradient Approximation Made Simple". *Phys. Rev. Lett.* **1998**, *80*, 890–890.

(54) Mardirossian, N.; Head-Gordon, M. Mapping the Genome of Meta-Generalized Gradient Approximation Density Functionals: The Search for B97M-V. *J. Chem. Phys.* **2015**, *142*, 074111.

(55) Najibi, A.; Goerigk, L. The Nonlocal Kernel in van der Waals Density Functionals as an Additive Correction: An Extensive Analysis with Special Emphasis on the B97M-V and ωB97M-V Approaches. *J. Chem. Theory Comput.* **2018**, *14*, 5725–5738.

(56) Najibi, A.; Goerigk, L. DFT-D4 Counterparts of Leading Meta-Generalized-Gradient Approximation

and Hybrid Density Functionals for Energetics and Geometries. *J. Comput. Chem.* **2020**, *41*, 2562–2572.

(57) Zhao, Y.; Truhlar, D. G. A New Local Density Functional for Main-Group Thermochemistry, Transition Metal Bonding, Thermochemical Kinetics, and Noncovalent Interactions. *J. Chem. Phys.* **2006**, *125*, 194101.

(58) Yu, H. S.; He, X.; Truhlar, D. G. MN15-L: A New Local Exchange-Correlation Functional for Kohn-Sham Density Functional Theory with Broad Accuracy for Atoms, Molecules, and Solids. *J. Chem. Theory Comput.* **2016**, *12*, 1280–1293.

(59) Furness, J. W.; Kaplan, A. D.; Ning, J.; Perdew, J. P.; Sun, J. Accurate and Numerically Efficient r^{2}SCAN Meta-Generalized Gradient Approximation. *J. Phys. Chem. Lett.* **2020**, *11*, 8208–8215.

(60) Ehlert, S.; Huniar, U.; Ning, J.; Furness, J. W.; Sun, J.; Kaplan, A. D.; Perdew, J. P.; Brandenburg, J. G. r^{2}SCAN-D4: Dispersion Corrected Meta-Generalized Gradient Approximation for General Chemical Applications. *J. Chem. Phys.* **2021**, *154*, 061101.

(61) Perdew, J. P.; Ruzsinszky, A.; Csonka, G. I.; Constantin, L. A.; Sun, J. Workhorse Semilocal Density Functional for Condensed Matter Physics and Quantum Chemistry. *Phys. Rev. Lett.* **2009**, *103*, 026403.

(62) Perdew, J. P.; Ruzsinszky, A.; Csonka, G. I.; Constantin, L. A.; Sun, J. Erratum: Workhorse Semilocal Density Functional for Condensed Matter Physics and Quantum Chemistry [Phys. Rev. Lett. **103** , 026403 (2009)]. *Phys. Rev. Lett.* **2011**, *106*, 179902.

(63) Tao, J.; Perdew, J. P.; Staroverov, V. N.; Scuseria, G. E. Climbing the Density Functional Ladder: Nonempirical Meta-Generalized Gradient Approximation Designed for Molecules and Solids. *Phys. Rev. Lett.* **2003**, *91*, 146401.

(64) Becke, A. D. Density-Functional Thermochemistry. III. The Role of Exact Exchange. *J. Chem. Phys.* **1993**, *98*, 5648–5652.

(65) Stephens, P. J.; Devlin, F. J.; Chabalowski, C. F.; Frisch, M. J. Ab Initio Calculation of Vibrational Absorption and Circular Dichroism Spectra Using Density Functional Force Fields. *J. Phys. Chem.* **1994**, *98*, 11623–11627.

(66) Becke, A. D. A New Mixing of Hartree-Fock and Local Density-Functional Theories. *J. Chem. Phys.* **1993**, *98*, 1372–1377.

(67) Yanai, T.; Tew, D. P.; Handy, N. C. A New Hybrid Exchange-Correlation Functional Using the Coulomb-Attenuating Method (CAM-B3LYP). *Chem. Phys. Lett.* **2004**, *393*, 51–57.

(68) Zhao, Y.; Truhlar, D. G. The M06 Suite of Density Functionals for Main Group Thermochemistry, Thermochemical Kinetics, Noncovalent Interactions, Excited States, and Transition Elements: Two New Functionals

and Systematic Testing of Four M06-Class Functionals and 12 Other Functionals. *Theor. Chem. Acc.* **2008**, *120*, 215–241.

(69) Grimme, S.; Brandenburg, J. G.; Bannwarth, C.; Hansen, A. Consistent Structures and Interactions by Density Functional Theory with Small Atomic Orbital Basis Sets. *J. Chem. Phys.* **2015**, *143*, 054107.

(70) Mardirossian, N.; Head-Gordon, M. ωB97M-V: A Combinatorially Optimized, Range-Separated Hybrid, Meta-GGA Density Functional with VV10 Nonlocal Correlation. *J. Chem. Phys.* **2016**, *144*, 214110.

(71) Mardirossian, N.; Head-Gordon, M. ωB97X-V: A 10-Parameter, Range-Separated Hybrid, Generalized Gradient Approximation Density Functional with Nonlocal Correlation, Designed by a Survival-of-the-Fittest Strategy. *Phys. Chem. Chem. Phys.* **2014**, *16*, 9904.

(72) Grimme, S. Semiempirical Hybrid Density Functional with Perturbative Second-Order Correlation. *J. Chem. Phys.* **2006**, *124*, 034108.

(73) Santra, G.; Sylvetsky, N.; Martin, J. M. L. Minimally Empirical Double-Hybrid Functionals Trained against the GMTKN55 Database: revDSD-PBEP86-D4, revDOD-PBE-D4, and DOD-SCAN-D4. *J. Phys. Chem. A* **2019**, *123*, 5129–5143.

(74) Goerigk, L.; Grimme, S. Efficient and Accurate Double-Hybrid-Meta-GGA Density Functionals—Evaluation with the Extended GMTKN30 Database for General Main Group Thermochemistry, Kinetics, and Noncovalent Interactions. *J. Chem. Theory Comput.* **2011**, *7*, 291–309.

(75) Alipour, M. Seeking for Spin-Opposite-Scaled Double-Hybrid Models Free of Fitted Parameters. *J. Phys. Chem. A* **2016**, *120*, 3726–3730.

(76) Mehta, N.; Casanova-Páez, M.; Goerigk, L. Semi-Empirical or Non-Empirical Double-Hybrid Density Functionals: Which Are More Robust? *Phys. Chem. Chem. Phys.* **2018**, *20*, 23175–23194.

(77) Casanova-Páez, M.; Dardis, M. B.; Goerigk, L. ωB2PLYP and ωB2GPPLYP: The First Two Double-Hybrid Density Functionals with Long-Range Correction Optimized for Excitation Energies. *J. Chem. Theory Comput.* **2019**, *15*, 4735–4744.

(78) Najibi, A.; Casanova-Páez, M.; Goerigk, L. Analysis of Recent BLYP- and PBE-Based Range-Separated Double-Hybrid Density Functional Approximations for Main-Group Thermochemistry, Kinetics, and Noncovalent Interactions. *J. Phys. Chem. A* **2021**, *125*, 4026–4035.

(79) Chai, J.-D.; Head-Gordon, M. Long-Range Corrected Double-Hybrid Density Functionals. *J. Chem. Phys.* **2009**, *131*, 174105.

(80) Caldeweyher, E.; Bannwarth, C.; Grimme, S. Extension of the D3 Dispersion Coefficient Model. *J. Chem. Phys.* **2017**, *147*, 034112.

(81) Lehtola, S.; Steigemann, C.; Oliveira, M. J.; Marques, M. A. Recent Developments in Libxc — A Comprehensive Library of Functionals for Density Functional Theory. *SoftwareX* **2018**, *7*, 1–5.

(82) Vydrov, O. A.; Van Voorhis, T. Nonlocal van Der Waals Density Functional: The Simpler the Better. *J. Chem. Phys.* **2010**, *133*, 244103.

(83) Wappett, D. A.; Goerigk, L. Erratum to "Toward a Quantum-Chemical Benchmark Set for Enzymatically Catalyzed Reactions: Important Steps and Insights". *J. Phys. Chem. A* **2020**, *124*, 1062–1062.

TOC Graphic